ACS APPLIED MATERIALS & INTERFACES

Research Article

www.acsami.org

Highly Efficient and Stable Electron Injection Layer for Inverted Organic Light-Emitting Diodes

Jun Liu,† Xinkai Wu,† Xindong Shi, Jing Wang, Zhiyuan Min, Yang Wang, Meijun Yang, and Gufeng He*

National Engineering Lab for TFT-LCD Materials and Technologies, and Department of Electronic Engineering, Shanghai Jiao Tong University, Shanghai 200240, People's Republic of China

ABSTRACT: A highly efficient and stable electron injection layer (EIL) for inverted organic light-emitting diodes (OLEDs) is developed. A 1 nm-thick Al is deposited between indium tin oxide cathode and commonly used Cs_2CO_3 EIL, which can significantly improve the stability. The Al may react with evaporated Cs_2CO_3 and form a much stabler Al−O−Cs complex, avoiding Cs oxidization by air according to X-ray photoemission spectroscopy measurement. When the Al is evaporated after Cs_2CO_3 layer, although such a Al−O−Cs complex also forms, the inferior electron injection at Al/4,7-diphenyl-1,10-phenanthroline interface leads to a joule heat-induced resistance that adversely affects the air stability of the device. It is expected that the developed Al/Cs_2CO_3 EIL promotes high efficiency and stable active-matrix OLEDs based on n-type thin film transistor.

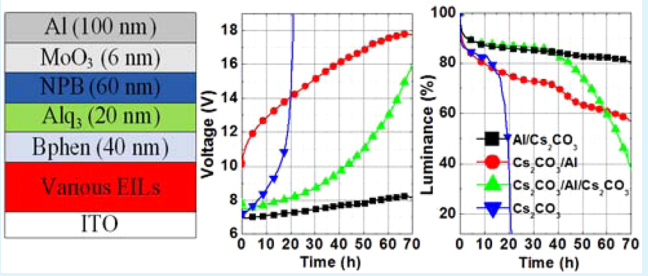

KEYWORDS: *high efficiency, air stability, electron injection layer, inverted OLED*

INTRODUCTION

Active matrix organic light-emitting diode (AMOLED)[1,2] has been commercialized in smart phones and TVs produced by Samsung and LG. Currently, the backplane of AMOLED is fabricated on the basis of a low temperature poly silicon-thin film transistor (LTPS-TFT) array, due to the high mobility and stability of LTPS.[3,4] However, LTPS fabrication requires an excimer-laser annealing (ELA) process, which results in nonuniformity and deteriorates production yield, especially for large size panels. On the other hand, indium gallium zinc oxide (IGZO)-TFT for AMOLED is an attractive alternative because it provides unique advantages of uniformity, large area, and low cost.[5,6] The n-type nature of IGZO promotes integration of IGZO-TFT and inverted OLED with a bottom cathode, to maintain the stability of OLED driven by the voltage controlled current source.[7−9] Because of the high optical transparency and electrical conductivity, indium tin oxide (ITO) is widely used as a cathode of inverted OLED. However, its high work function limits electron injection into the neighboring electron-transporting layer (ETL). Bulk n-type doped ETL by alkali metals or their compounds[10−12] (e.g., Li, Cs, Rb_2CO_3, Cs_2CO_3) are usually sandwiched between ITO and undoped ETL to facilitate electron injection from ITO. To simplify the fabrication, on the other hand, an ultrathin interlayer[13−15] such as LiF, Liq, and Cs_2CO_3 is often used as the electron-injecting layer (EIL). Such EILs have been proved to possess excellent electron injecting property, but they readily decompose to alkali metals that are prone to be oxidized in air, leading to long-term instability. Recently, solution processed conjugated polyelectrolytes[16] or n-type metal oxides such as zinc oxide (ZnO),[17] titanium dioxide (TiO_2),[18] tin dioxide (SnO_2),[19] and zirconium dioxide (ZrO_2)[20] have been developed as promising candidates for air-stable EIL. However, these metal oxides fabricated by the sol−gel method require a high annealing temperature over 300 °C for better electron injecting ability, and complete coverage of metal oxide with large surface roughness needs enough thick ETL, which will lead to high operating voltages. Although metal oxide can be deposited by sputtering at relatively low temperature, using sputtered metal oxide as EILs in organic optoelectronic devices such as OLED and organic photovoltaic cell (OPV) is rarely reported. Thermal evaporation of alkali metal compound such as Cs_2CO_3 powder is simple and easily controlled, and the subsequent deposition of organic layers is continuously accomplished in one chamber. On the contrary, sputtering metal oxide requires additional equipment and complex processes. Besides, the cost of Cs_2CO_3 powder is significantly lower than that of the metal oxide target. Therefore, thermal evaporation of alkali metal compound as EIL is more preferable in the OLED field, especially for research. For inverted OLED, it is still important and urgent to develop stable and easily fabricated EIL.

Here, the widely used EIL Cs_2CO_3 is modified to develop highly efficient and stable EIL for inverted device. Unlike the commonly used EIL LiF or Liq that requires the reaction with Al to liberate Li atoms, the thermal evaporated Cs_2CO_3 does not need an external metal layer to produce Cs, because decomposition of evaporated Cs_2CO_3 to Cs is thermodynami-

Received: September 14, 2014
Accepted: March 6, 2015
Published: March 6, 2015

DOI: 10.1021/am506300c
ACS Appl. Mater. Interfaces 2015, 7, 6438−6443

cally allowed.[21] However, by depositing an ultrathin Al between ITO and Cs_2CO_3, the instability of the evaporated Cs_2CO_3 layer because of easy oxidation of Cs is significantly improved. To investigate the functionality of the thin Al layer, it is inserted at various positions in the device and analyzed by their surface electronic properties and work functions.

EXPERIMENTAL SECTION

The inverted devices were fabricated on ITO-coated glass substrates. Prior to film deposition, the ITO glass substrates were cleaned successively using deionized water, acetone, and isopropanol under an ultrasonic bath, and then treated with UV-ozone after drying. The devices with four kinds of EILs, Cs_2CO_3 (1 nm), Al (1 nm)/Cs_2CO_3 (1 nm), Cs_2CO_3 (1 nm)/Al (1 nm), and Cs_2CO_3 (1 nm)/Al (1 nm)/Cs_2CO_3 (1 nm), were fabricated. For fabrication of Al/Cs_2CO_3 and Cs_2CO_3/Al on ITO, Al and Cs_2CO_3 were first deposited on ITO, respectively. As shown in Figure 1, the structure of the device is ITO/

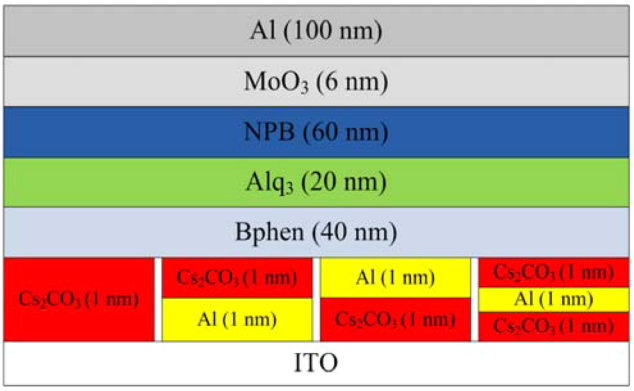

Figure 1. Device structures of inverted OLEDs with various EILs: Cs_2CO_3 (1 nm), Al (1 nm)/Cs_2CO_3 (1 nm), Cs_2CO_3 (1 nm)/Al (1 nm), and Cs_2CO_3 (1 nm)/Al (1 nm)/Cs_2CO_3 (1 nm).

EIL/ETL (40 nm)/emission layer (EML) (20 nm)/hole transporting layer (HTL) (60 nm)/hole injection layer (HIL) (6 nm)/Al (100 nm), where ETL, EML, HTL, and HIL are BPhen, Alq_3, *N*,*N*-di(1-naphthyl)-*N*,*N*-diphenyl-(1,1′-biphenyl)-4,4′-diamine (NPB), and MoO_3, respectively.

The EIL, ETL, EML, HTL, HIL, and anode Al were thermally deposited in a high vacuum deposition system at a base pressure of 10^{-6} Torr. The deposition rate for organic materials was detected by quartz-crystal monitors within the range from 0.01 to 0.1 nm/s. The devices' current density−voltage (*J*−*V*) and luminance−voltage (*L*−*V*) characteristics were measured with a computer controlled Keithley 2400 source meter and BM-7A luminance colorimeter immediately after finishing fabrication without encapsulation under ambient conditions. Because we can get four identical devices on one substrate, the remaining untested devices were used to test their voltage rise and luminance decay. The devices for stability test were operated at a fixed current density of 10 mA/cm^2. X-ray and ultraviolet photoemission spectroscopy (XPS and UPS) measurements were carried out in a Kratos AXIS UltraDLD ultrahigh vacuum surface analysis system with a monochromatic aluminum Kα source (1486.6 eV) and a He I (21.2 eV) gas discharge lamp, respectively.

RESULTS AND DISCUSSION

Cs_2CO_3 has been widely used to facilitate electron injection from ITO to ETL in inverted OLED. However, whether ITO/Cs_2CO_3 interface or Cs_2CO_3/ETL interface dominates the electron injection requires further study. To address this question, an ultrathin Al layer was deposited before or after Cs_2CO_3 layer to investigate the effects of Al on electron injection from ITO to ETL. As shown in Figure 2, all devices

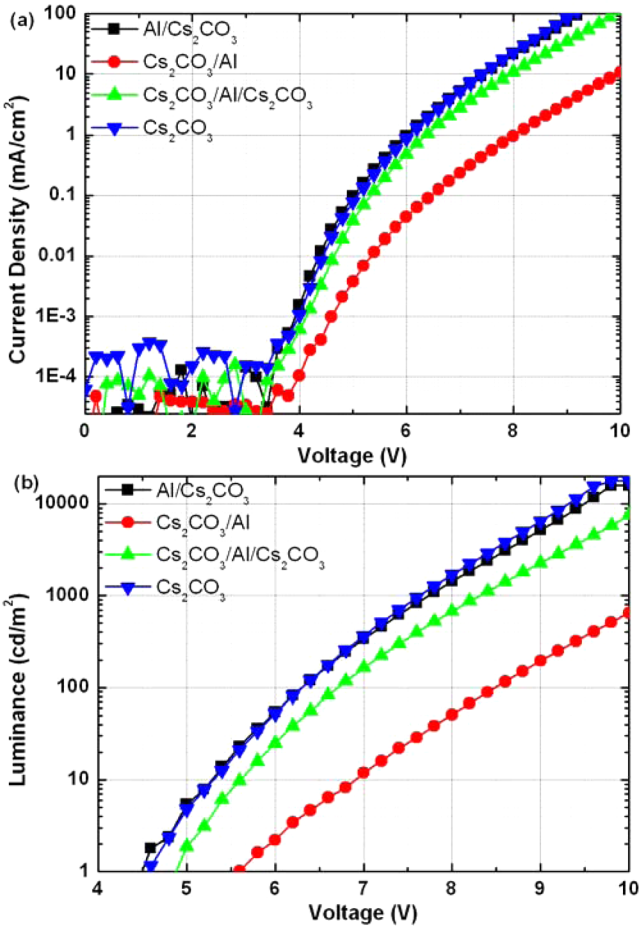

Figure 2. Current density−voltage (a) and luminance−voltage (b) characteristics of inverted devices with various EILs.

with Cs_2CO_3 EIL directly contacting BPhen layer behave very similarly, whereas their current densities and luminance are significantly larger than those of the device with Al inserted between Cs_2CO_3 and BPhen layer. For example, at a current density of 10 mA/cm^2, the driving voltage of the Cs_2CO_3-based device is about 7.2 V, while that of the Cs_2CO_3/Al-based device is about 10 V. The turn-on voltage (V_{on}) for 1 cd/m^2 of the Cs_2CO_3-based device is 4.5 V, while that of the Cs_2CO_3/Al-based device is 5.5 V. This indicates that the Cs_2CO_3/BPhen interface has superior electron injection property than (Cs_2CO_3/Al)/BPhen interface. The favorable electron injection by Cs_2CO_3/BPhen interface is attributed to the n-type doped BPhen by Cs_2CO_3 at the interface. The electron transfer from Cs_2CO_3 to BPhen leads to a shift of Fermi level to the lowest unoccupied molecular orbital (LUMO) of BPhen.[22] The subsequent deposition of Al on top of Cs_2CO_3 impedes charge transfer at the Cs_2CO_3/BPhen interface, resulting in inferior electron injection for the device with Cs_2CO_3/Al EIL. For the device with Al/Cs_2CO_3 EIL, it exhibits *J*−*V* and *L*−*V* characteristics almost identical to those of the device without Al, indicating a negligible effect of ultrathin layer Al between ITO and Cs_2CO_3 on electron injection. This further demonstrates that Cs_2CO_3/ETL interface instead of ITO/Cs_2CO_3 interface dominates electron injection for the inverted device. The deteriorated electron injection property for Cs_2CO_3/Al can be healed by adding another Cs_2CO_3 layer on top of Cs_2CO_3/Al bilayer. As compared to the device with

DOI: 10.1021/am506300c
ACS Appl. Mater. Interfaces 2015, 7, 6438−6443

Cs_2CO_3/Al, the device with Cs_2CO_3/Al/Cs_2CO_3 displays dramatically increased current density and reduced turn-on voltage, which approaches $J-V$ and $L-V$ characteristics of the device with EIL Cs_2CO_3 or Al/Cs_2CO_3.

Figure 3 compares the CE and power efficiency (PE) of inverted devices with various EILs. At the same current density,

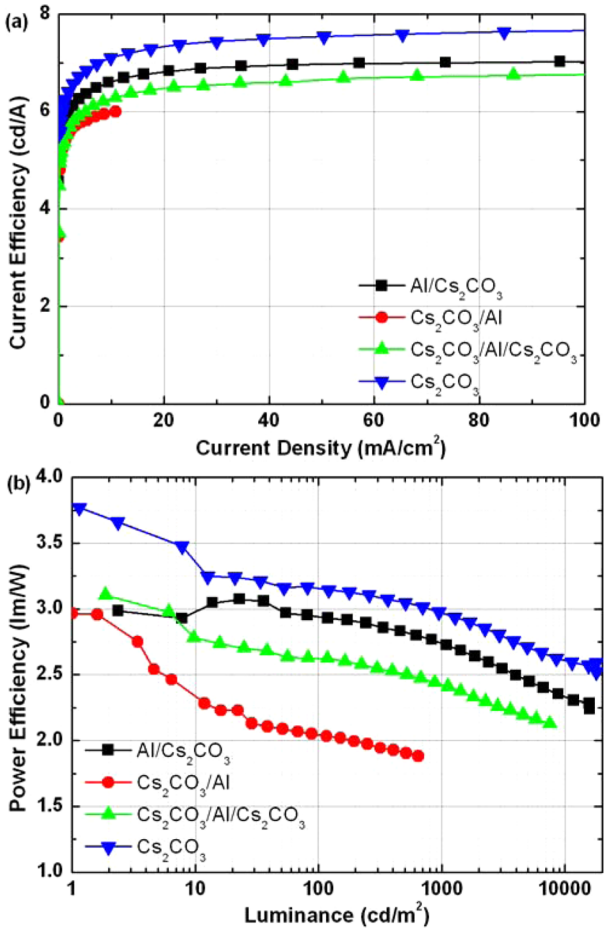

Figure 3. Current efficiency–current density (a) and power efficiency–luminance (b) characteristics of inverted devices with various EILs.

the device with Cs_2CO_3/Al EIL shows the lowest CE and PE. Because of the superior hole injection ability of MoO_3 top-contact and the inferior electron injection ability of Cs_2CO_3/Al, a larger amount of holes than electrons are transported into the Alq_3 emitter, and excess holes produce unstable Alq^{3+} cations that lead to excitons quenching. This is responsible for low CE for device with Cs_2CO_3/Al as EIL, and also its inferior electron injection determines the low PE of device with high driving voltage. As electron injection ability of EIL increases, recombination of holes and electrons is balanced and the formation of unstable Alq^{3+} cations is suppressed, resulting in enhanced CE of the device. The device with Al/Cs_2CO_3 EIL achieves an increased CE of about 7.0 cd/A, and that with Cs_2CO_3 EIL has the largest CE of about 7.5 cd/A. To the best of our knowledge, such CE values are among the highest values ever reported for a Alq_3-based device. Moreover, the current efficiencies of all inverted devices grow with current density until they tend to saturation at a current density larger than 20 mA/cm^2. Because the hole injection ability of MoO_3 top-contact is larger than the electron injection ability of bottom-contact Cs_2CO_3, holes are favorably injected and accumulated at the BPhen/Alq_3 interface, resulting in recombination location at the BPhen/Alq_3 interface at low driving voltage. As the driving voltage increased, electron injection from ITO is enhanced. This leads to the extended recombination zone into the Alq_3 bulk layer, resulting in higher CE at higher driving voltage. As shown in Figure 3, the PE of the proposed EIL Al/Cs_2CO_3-based device is slightly lower than that of the Cs_2CO_3-based device, which is not attributed to poorer electron injection property of Al/Cs_2CO_3. Actually, even slightly higher current is observed with Al/Cs_2CO_3 EIL in Figure 2. The slightly lower PE may be due to the change of charge carrier balance. On the other hand, such a small difference (<10%) could also result from process or measurement variation.

Besides the electron injection property of EIL, its long-term stability is also an important issue. We have evaluated the voltage rise and luminance decay of inverted devices with various EILs at a fixed current density of 10 mA/cm^2. All of the devices were exposed in ambient condition without encapsulation. The inverted device without encapsulation is to accelerate the degradation process to compare the stability of Al/Cs_2CO_3 and Cs_2CO_3 EIL. Although encapsulation can protect the device from being oxidized, the water and oxygen still penetrate into the device even with the encapsulation technique state of the art, especially with the thin film encapsulation for flexible device. As shown in Figure 4, during a 21 h operation test, the device with Cs_2CO_3 EIL shows significantly increased driving voltage by 12 V, and its

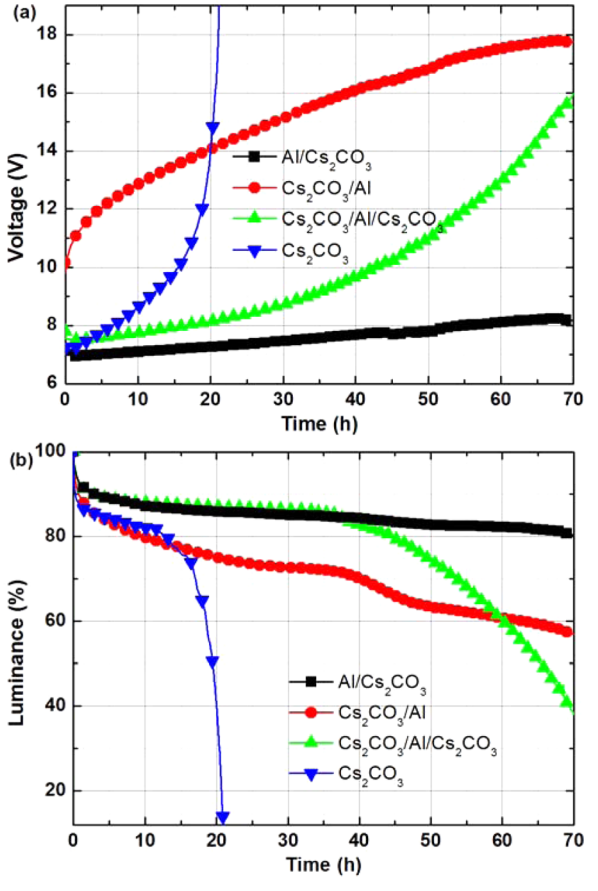

Figure 4. Voltage rise (a) and luminance decay (b) of inverted devices with various EILs.

DOI: 10.1021/am506300c
ACS Appl. Mater. Interfaces 2015, 7, 6438–6443

luminance seriously drops to 10% of the initial value. This indicates that the electron injection barrier between ITO and the thermal evaporated Cs_2CO_3 layer gradually increases with time. The thermal evaporated Cs_2CO_3 was reported to decompose metallic Cs rather than into Cs_2O. The low work function of Cs with 1.9 eV renders it easily oxidized by water and oxygen. If the evaporated Cs_2CO_3 on the ITO substrate is pristine or decomposes to Cs_2O, the inverted device should not have a badly deteriorated performance, as Cs_2CO_3 or Cs_2O is hardly oxidized by oxygen.[23] Therefore, the oxidation of Cs in air contributes to the instability of thermal evaporated Cs_2CO_3. However, the ultrathin Al layer deposited between ITO and Cs_2CO_3 may prevent oxidation of Cs. Although Al/Cs_2CO_3 and Cs_2CO_3 possess almost identical electron injection properties, the stability of Al/Cs_2CO_3 is significantly superior to that of Cs_2CO_3. During 70 h operation test, the driving voltage rise of device with EIL Al/Cs_2CO_3 is just about 1 V, and the luminance of that decays to 80% of its initial value. The high stability of the Al/Cs_2CO_3-based device should be originated from the Al−O−Cs complex[24] produced by chemical reaction of subsequent evaporated Cs_2CO_3 and underlying Al. As compared to the metallic Cs, the Al−O−Cs complex is less prone to be oxidized by oxygen. For Cs_2CO_3/Al EIL, the evaporation of Al on top of Cs_2CO_3 can also lead to the Al−O−Cs complex, leading to better stability of Cs_2CO_3/Al EIL than that of Cs_2CO_3 EIL. However, the device with Cs_2CO_3/Al EIL exhibits larger voltage rise, as compared to that with Al/Cs_2CO_3 EIL. This is related to distinctly different electron injection properties of Cs_2CO_3/Al and Al/Cs_2CO_3 as shown in Figure 2. Because of the weak electron injection capability of Cs_2CO_3/Al, a large amount of electrons accumulates at the (Cs_2CO_3/Al)/BPhen interface, leading to excess joule heat at such interface. This will damage the adjacent organic layer BPhen with low glass transition temperature, resulting in increased resistance and large voltage rise of the device. Conversely, the joule heat-induced resistance is suppressed in the Al/Cs_2CO_3-based device with excellent electron injection property. Because the Al−O−Cs complex forms in both EILs, the question that why devices with EIL Cs_2CO_3/Al and Al/Cs_2CO_3 exhibit distinctly different characteristics as shown in Figure 2 is raised. We present the reason as follows. The cover of Al on Cs_2CO_3 or Cs_2CO_3 on Al does not completely convert to Al−O−Cs complex, leaving original Al or Cs_2CO_3 to form Al/BPhen or Cs_2CO_3/BPhen interface. The deposition of another Cs_2CO_3 on top of Cs_2CO_3/Al produces a new Cs_2CO_3/BPhen interface, but the second evaporated Cs_2CO_3 layer mainly stays pristine because most of the Al has reacted with the underlying evaporated Cs_2CO_3. This contributes to high voltage rise for the device with EIL $Cs_2CO_3/Al/Cs_2CO_3$.

To further understand the mechanism for the higher stability of Al/Cs_2CO_3 than Cs_2CO_3, the evaporated Al/Cs_2CO_3 and Cs_2CO_3 films on top of ITO have been studied by XPS, as shown in Figure 5. The films were exposed in air for about 10 min prior to the measurements. Because of the highly reactive and catalytic Cs from evaporated Cs_2CO_3, oxygenated chemicals such as H_2O, CO_2, and O_2 in air can easily adsorb on Cs to induce a complicated hydroxylation and carbonylation reaction,[25] which correspond to the C1 speaks at 286.1 and 288.1 eV for evaporated Cs_2CO_3 film, respectively. That is why evaporated Cs_2CO_3 exhibits deteriorated electron injection stability in air. However, the intensities of C 1s peaks at 286.1 and 288.1 eV for Al/Cs_2CO_3 are reduced, referring that the

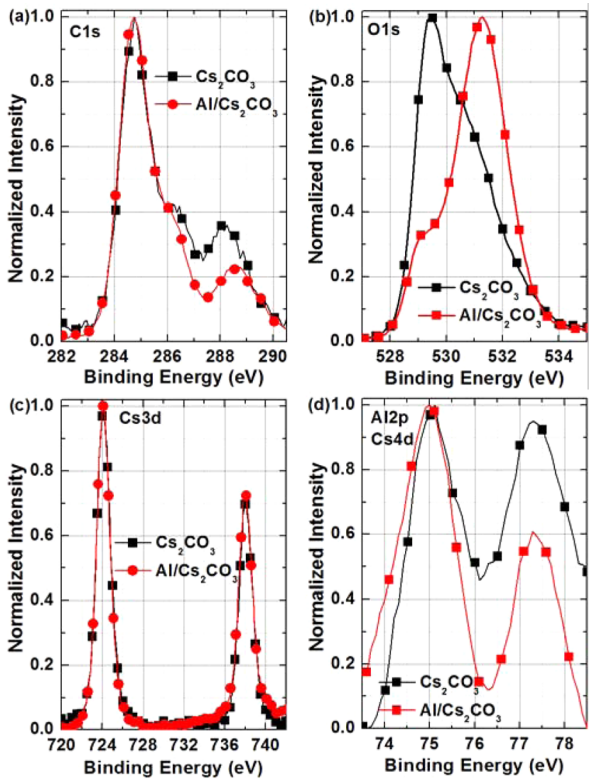

Figure 5. C 1s (a), O 1s (b), Cs 3d (c), and Al 2p and Cs 4d (d) spectra of Cs_2CO_3 and Al/Cs_2CO_3 films exposed in air for about 10 min.

induced chemical reaction on Cs is suppressed by Al. The reaction of Al with the subsequent evaporated Cs_2CO_3 should prevent further catalysis reaction on the latter. As shown in Figure 5d, the Al 2p band and the Cs 4d band are overlapped, and the binding energy at 74 eV indicates oxidized Al. Moreover, as compared to those for pristine Cs,[22] the Cs 3d peaks for Al/Cs_2CO_3 are shifted to lower binding energies at 724.1 and 738.1 eV, indicating oxidized Cs in Al/Cs_2CO_3 film. Therefore, the product for Al/Cs_2CO_3 is speculated to be Al−O−Cs complex[24] that also possesses excellent electron injection property. Although both Cs 3d peaks for Al/Cs_2CO_3 and Cs_2CO_3 are almost identical, the products of oxidization of Cs for Al/Cs_2CO_3 and Cs_2CO_3 films are different. For O 1s spectra, they show two characteristic peaks, which should be assigned to the ITO at 529.3 eV and oxidized Cs or Al at 531.3 eV, respectively. The dominated O 1s peak at 531.3 eV for Al/Cs_2CO_3 indicates that the Al−O−Cs complex is formed on ITO. Because of the reduced catalysis and reactivity of the Al−O−Cs complex, it is hard to further oxidize. As a result, the Al/Cs_2CO_3 film shows efficient and stable electron injection ability.

UPS has been used to measure the work functions of bare ITO and ITO modified by Cs_2CO_3, Cs_2CO_3/Al, $Cs_2CO_3/Al/Cs_2CO_3$, and Al/Cs_2CO_3. Because of unavoidable air exposure of samples loaded into test equipment in our lab, the measured work functions are not for the pristine EILs, but reflect the air stability of EILs. As shown in Figure 6b, the photoemission onsets of ITO, ITO/Cs_2CO_3, ITO/Cs_2CO_3/Al, $ITO/Cs_2CO_3/Al/Cs_2CO_3$, and $ITO/Al/Cs_2CO_3$ are found at 17.03, 17.08, 18.07, 17.69, and 17.82, which correspond to the work functions of 4.17, 4.12, 3.13, 3.51, and 3.38 eV, respectively. The evaporated Cs_2CO_3 has been proved to be an efficient EIL,

DOI: 10.1021/am506300c
ACS Appl. Mater. Interfaces 2015, 7, 6438−6443

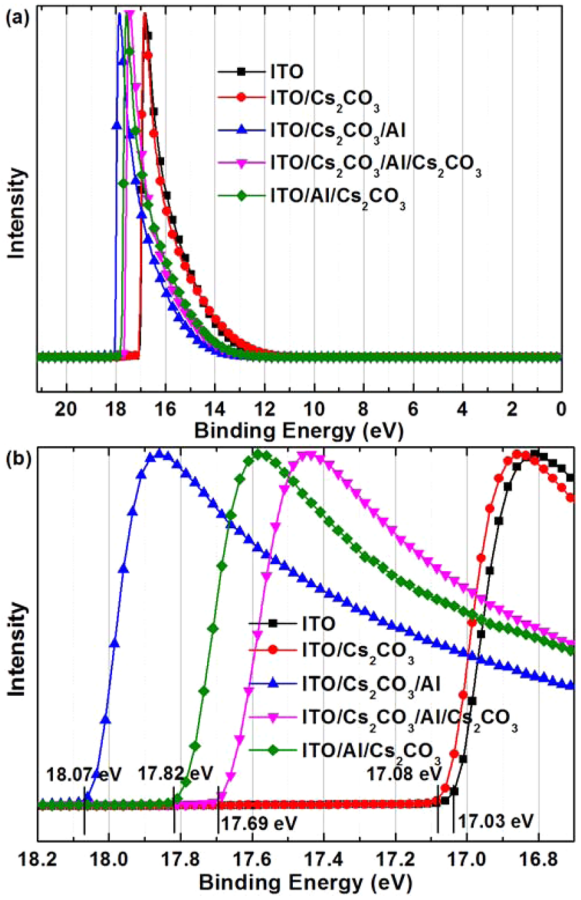

Figure 6. UPS spectra of air-exposed ITO and ITO modified by different EILs: (a) the full UPS spectrum using He I radiation, and (b) secondary-electron cutoff.

and the work function of ITO/Cs_2CO_3 was about 0.4 eV[26] or even 1.0 eV[15] lower than that of ITO in previous reports. However, an almost identical work function in our measurement indicates the invalid electron injection of Cs_2CO_3 by air exposure, and further proves that the evaporated Cs_2CO_3 is unstable. The 1 nm Al deposition on or beneath Cs_2CO_3 can produce Al−O−Cs complex, providing enhanced air stability, and their work functions remain lower than that of ITO even exposed to air. However, their electron injection properties are quite different. The current density of the ITO/Cs_2CO_3/Al-based device is much lower than that of the ITO/Al/Cs_2CO_3-based device, although ITO/Cs_2CO_3/Al has a lower work function, indicating that the n-type doped Cs_2CO_3/BPhen interface instead of work function of EIL-modified ITO dominates electron injection from ITO to BPhen. When depositing another thin layer of Cs_2CO_3 on top of ITO/Cs_2CO_3/Al, the current density is greatly enhanced, although the work function is higher, which further confirms the importance of the Cs_2CO_3/BPhen interface for electron injection. Comparing Al/Cs_2CO_3 and Cs_2CO_3/Al/Cs_2CO_3, because both devices have the n-type doping at the Cs_2CO_3/BPhen interface, the higher current density of the Al/Cs_2CO_3-based device is mainly originated from the lower work function of ITO/Al/Cs_2CO_3 than that of ITO/Cs_2CO_3/Al/Cs_2CO_3.

CONCLUSION

In summary, we have developed a highly efficient and stable Al/Cs_2CO_3 EIL for inverted OLEDs. The device with such EIL shows almost identical $J-V$ and $L-V$ characteristics with the common Cs_2CO_3-only EIL device, due to the favorable electron injection for the same Cs_2CO_3/BPhen interfaces. The inverted devices using Alq_3 as EML achieve current efficiencies of 7.0 and 7.5 cd/A when Al/Cs_2CO_3 and Cs_2CO_3 are employed as EIL, respectively. To the best of our knowledge, such efficiencies are among the highest values ever reported for an Alq_3-based device. However, due to the fast oxidation of Cs decomposed from the evaporated Cs_2CO_3, Cs_2CO_3-based device without encapsulation shows seriously deteriorated stability with a voltage rise of more than 12 V and luminance decay of 90% after 21 h operation. On the contrary, Al/Cs_2CO_3-based device without encapsulation shows a voltage rise of only 1 V after 70 h operation in ambient condition. According to the XPS analysis on Al/Cs_2CO_3 and Cs_2CO_3, the complicated hydroxylation and carbonylation reaction on evaporated Cs_2CO_3 can be suppressed by inserted Al. We attribute the enhanced long-term stability of Al/Cs_2CO_3 to the stable Al−O−Cs complex that is a product of evaporated Cs_2CO_3 reacting with the underlying Al. The Al−O−Cs complex can also be produced by evaporating 1 nm Al between Cs_2CO_3 and ETL, while the inferior electron injection at the Al/BPhen interface results in the joule heat-induced resistance at the interface. On the basis of our results, it is anticipated that the EIL Al/Cs_2CO_3 will facilitate the development of highly efficient and stable inverted AMOLED.

AUTHOR INFORMATION

Corresponding Author

*Tel.: +86-21-34207045. Fax: +86-21-34204371. E-mail: gufenghe@sjtu.edu.cn.

Author Contributions

†J.L. and X.W. contributed equally.

Notes

The authors declare no competing financial interest.

ACKNOWLEDGMENTS

We thank the 973 Program (2013CB328803, 2013CB328804), the National Natural Science Foundation of China (61377030), and the Science and Technology Commission of Shanghai Municipal (12JC1404900) for financial support. We thank Qianqian Hu and Limin Sun from the Instrumental Analysis Center of SJTU for XPS and UPS measurements, respectively.

REFERENCES

(1) Helander, M. G.; Wang, Z. B.; Qiu, J.; Greiner, M. T.; Puzzo, D. P.; Liu, Z. W.; Lu, Z. H. Chlorinated Indium Tin Oxide Electrodes with High Work Function for Organic Device Compatibility. *Science* **2011**, *332*, 944−947.

(2) Reineke, S.; Lindner, F.; Schwartz, G.; Seidler, N.; Walzer, K.; Lüssem, B.; Leo, K. White Organic Light-Emitting Diodes with Fluorescent Tube Efficiency. *Nature* **2009**, *459*, 234−238.

(3) Jeong, J. K.; Jeong, J. H.; Yang, H. W.; Ahn, T. K.; Kim, M.; Kim, K. S.; Gu, B. S.; Chung, H. J.; Park, J. S.; Mo, Y. G. 12.1-in. WXGA AMOLED Display Driven by InGaZnO Thin-Film Transistor. *J. Soc. Inf. Disp.* **2009**, *17*, 95−100.

(4) Jung, S. H.; Nam, W. J.; Han, M. K. A New Voltage-Modulated AMOLED Pixel Design Compensating for Threshold Voltage Variation in Poly-Si TFTs. *IEEE Electron Device Lett.* **2004**, *25*, 690−692.

(5) Nomura, K.; Ohta, H.; Takagi, A.; Kamiya, T.; Hirano, M.; Hosono, H. Room-Temperature Fabrication of Transparent Flexible Thin-Film Transistors Using Amorphous Oxide Semiconductors. *Nature* **2004**, *432*, 488−492.

DOI: 10.1021/am506300c
ACS Appl. Mater. Interfaces 2015, 7, 6438−6443

(6) Yamazki, S.; Koyama, J.; Yamamoto, Y.; Okamoto, K. Research, Development, and Application of Crystalline Oxide Semiconductor. *SID Int. Symp. Dig. Technol. Pap.* **2012**, *43*, 183−186.
(7) Chu, T.-Y.; Chen, J.-F.; Chen, S.-Y.; Chen, C.-J.; Chen, C. H. Highly Efficient and Stable Inverted Bottom-Emission Organic Light Emitting Devices. *Appl. Phys. Lett.* **2006**, *89*, 053503.
(8) Chu, T.-Y.; Chen, J.-F.; Chen, C. H. Ultrathin Electron Injection Layer on Indium-Tin Oxide Bottom Cathode for Highly Efficient Inverted Organic Light-Emitting Diodes. *Jpn. J. Appl. Phys.* **2006**, *45*, 4948−4950.
(9) Fukagawa, H.; Morii, K.; Arimoto, Y.; Nakata, M.; Nakajima, Y.; Shimizu, T.; Yamamoto, T. Highly Efficient Inverted OLED with Air-Stable Electron Injection Layer. *SID Int. Symp. Dig. Technol. Pap.* **2013**, *44*, 1466−1469.
(10) Zhou, X.; Pfeiffer, M.; Huang, J. S.; Blochwitz-Nimoth, J.; Qin, D. S.; Werner, A.; Drechsel, J.; Maenning, B.; Leo, K. Low-Voltage Inverted Transparent Vacuum Deposited Organic Light-Emitting Diodes Using Electrical Doping. *Appl. Phys. Lett.* **2002**, *81*, 922−924.
(11) Xiong, T.; Wang, F.; Qiao, X.; Ma, D. Cesium Hydroxide Doped Tris-(8-Hydroxyquinoline) Aluminum as an Effective Electron Injection Layer in Inverted Bottom-Emission Organic Light Emitting Diodes. *Appl. Phys. Lett.* **2008**, *92*, 263305.
(12) Lee, J.-H.; Wang, P.-S.; Park, H.-D.; Wu, C.-I.; Kim, J.-J. A High Performance Inverted Organic Light Emitting Diode Using an Electron Transporting Material with Low Energy Barrier for Electron Injection. *Org. Electron.* **2011**, *12*, 1763−1767.
(13) Chiba, T.; Pu, Y.-J.; Miyazaki, R.; Nakayama, K.-i.; Sasabe, H.; Kido, J. Ultra-High Efficiency by Multiple Emission from Stacked Organic Light-Emitting Devices. *Org. Electron.* **2011**, *12*, 710−715.
(14) Liu, J.; Wang, J.; Huang, S.; Shi, X.; Wu, X.; He, G. A Highly Efficient, Transparent and Stable Charge Generation Unit Based on a P-Doped Monolayer. *Org. Electron.* **2013**, *14*, 1337−1343.
(15) Chen, M.-H.; Wu, C.-I. The Role of Thermal Evaporated Cesium Carbonate to Enhance the Electron Injection in Organic Light Emitting Devices. *J. Appl. Phys.* **2008**, *104*, 113713.
(16) Chen, J.; Shi, C.; Fu, Q.; Zhao, F.; Hu, Y.; Feng, Y.; Ma, D. Solution-Processable Small Molecules as Efficient Universal Bipolar Host for Blue, Green and Red Phosphorescent Inverted OLEDs. *J. Mater. Chem.* **2012**, *22*, 5164−5170.
(17) Kabra, D.; Lu, L. P.; Song, M. H.; Snaith, H. J.; Friend, R. H. Efficient Single-Layer Polymer Light-Emitting Diodes. *Adv. Mater.* **2010**, *22*, 3194−3198.
(18) Bolink, H. J.; Coronado, E.; Repetto, D.; Sessolo, M.; Barea, E. M.; Bisquert, J.; Garcia-Belmonte, G.; Prochazka, J.; Kavan, L. Inverted Solution Processable OLEDs Using a Metal Oxide as an Electron Injection Contact. *Adv. Funct. Mater.* **2008**, *18*, 145−150.
(19) Lee, H.; Kang, C. M.; Park, M.; Kwak, J.; Lee, C. Improved Efficiency of Inverted Organic Light-Emitting Diodes Using Tin Dioxide Nanoparticles as an Electron Injection Layer. *ACS Appl. Mater. Interfaces* **2013**, *5*, 1977−1981.
(20) Tokmoldin, N.; Griffiths, N.; Bradley, D. D. C.; Haque, S. A. A Hybrid Inorganic-Organic Semiconductor Light-Emitting Diode Using ZrO_2 as an Electron-Injection Layer. *Adv. Mater.* **2009**, *21*, 3475−3478.
(21) Li, Y.; Zhang, D.-Q.; Duan, L.; Zhang, R.; Wang, L.-D.; Qiu, Y. Elucidation of the Electron Injection Mechanism of Evaporated Cesium Carbonate Cathode Interlayer for Organic Light-Emitting Diodes. *Appl. Phys. Lett.* **2007**, *90*, 012119.
(22) Cai, Y.; Wei, H. X.; Li, J.; Bao, Q. Y.; Zhao, X.; Lee, S. T.; Li, Y. Q.; Tang, J. X. Mechanism of Cs_2CO_3 as N-Type Dopant in Organic Electron-Transport Film. *Appl. Phys. Lett.* **2011**, *98*, 113304.
(23) Liu, Q.; Duan, L.; Li, Y.; Qiao, J.; Yu, Z.; Zhang, D.; Wang, L.; Dong, G.; Qiu, Y. Study on the Electron Injection Mechanism of Thermally Decomposable Cs_2CO_3. *Jpn. J. Appl. Phys.* **2009**, *48*, 102302.
(24) Huang, J.; Xu, Z.; Yang, Y. Low-Work-Function Surface Formed by Solution-Processed and Thermally Deposited Nanoscale Layers of Cesium Carbonate. *Adv. Funct. Mater.* **2007**, *17*, 1966−1973.
(25) Rodriguez, J. A.; Clendening, W. D.; Campbell, C. T. Adsorption of CO and CO_2 on Clean and Cesium-Covered Cu(110). *J. Phys. Chem.* **1989**, *93*, 5238−5248.
(26) Park, B.; Shin, J. C.; Cho, C. Y. Water-Processable Electron-Collecting Layers of a Hybrid Poly(ethylene oxide): Caesium Carbonate Composite for Flexible Inverted Polymer Solar Cells. *Sol. Energy Mater. Sol. Cells* **2013**, *108*, 1−8.

DOI: 10.1021/am506300c
ACS Appl. Mater. Interfaces 2015, 7, 6438−6443